

Liquefaction Assessment Based on Centrifuge CPTs

D. Giretti¹, V. Fioravante², C. Prearo³

ABSTRACT

The paper presents a semi-empirical method for the liquefaction assessment based on CPTs. The cone resistance q_c and the cyclic resistance CRR of a un-aged, un-cemented soil depend on the same properties: type of soil, fabric, stress level and density. The latter two quantities can be synthesized through the state parameter ψ , which in this paper is used to link q_c , measured via centrifuge CPTs, to CRR, derived from cyclic undrained triaxial tests. A relationship between the normalized cone resistance and ψ was calibrated from the results of 27 centrifuge CPTs on dry Ticino Sand (TS4) models. The results of 16 cyclic undrained triaxial tests on TS4 were interpreted to define a correlation between ψ and CRR at a given number of cycles N . The centrifuge and triaxial test results were combined to deduce a direct relationship between the normalized cone resistance and the CRR, which can be used for liquefaction assessment from field CPTs.

Introduction

The occurrence of liquefaction depends on the cyclic shear loading induced by an earthquake and on the cyclic resistance of the soil; the latter, due to the difficulties in obtaining undisturbed samples of most liquefiable soils, is usually deduced from field test results interpreted via empirical correlations which provide the link between cyclic resistance and test indices. The collection of a great number of field test data and observations of real occurrences allowed developing empirical approaches expressed as graphs, where the cyclic stress resistance is plotted versus the in situ test index. A bounding line defines two areas: one where liquefaction is possible and the other where liquefaction is not expected. Initially, the methods were based on the results of standard penetration tests (Seed and Idriss, 1982); then, as the SPT has been progressively replaced by the cone penetration test (more repeatable and reliable), CPT based methods of liquefaction assessment have become the most used in practice engineering (starting from Roberston and Campanella, 1985). Recently, methods based on the shear wave velocity profile have been developed (Andrus and Stokoe, 1997).

In general, the cone penetration resistance q_c and the cyclic resistance of a un-aged, un-cemented soil, depend on the material properties (i.e. mineralogy, shape, asperities and roughness of grains, grading and fabric) and the state of the soil, i.e. stress level and density. The latter two quantities can be expressed by the state parameter ψ (i.e. the distance along the void ratio axis, in the $e - p'$ plane, of a given state from the critical state line, Been and Jefferies, 1985), which is an indicator of the direction of volumetric strains (dilation or contraction) during shearing and so

¹Ph.D., ENDIF, University of Ferrara, Italy, daniela.giretti@unife.it

²Full Professor, ENDIF, University of Ferrara, Italy, vincenzo.fioravante@unife.it

³Ph.D., ENDIF, University of Ferrara, Italy, chiara.prearo@unife.it

can be used to link directly the tip resistance to the cyclic resistance. Here the results of centrifuge CPT tests and cyclic undrained triaxial tests carried out using the well-known Italian Ticino Sand (TS4) are presented. All the centrifuge and the triaxial tests, belong to the database of ISMGEO (Istituto Sperimentale Modelli Geotecnici, formerly ISMES, Seriate – BG – Italy).

The results of cone penetration tests were a simple exponential relationship between the normalized cone resistance Q_p and the state parameter ψ (Been et al., 1986). The cyclic triaxial test results were interpreted to define a correlation between the state parameter and the cyclic resistance ratio CRR at a given number of cycles N . Finally, results of centrifuge and triaxial tests have been combined to deduce a direct relationship between the normalized cone resistance and the cyclic resistance ratio.

Testing Soil, Program and Procedures

The soil used in this research is the well-known Italian Ticino Sand (TS4); the grain size distribution and the index properties are given in Figure 1. TS4 is a uniform coarse to medium sand made of angular to subrounded particles and composed of 30% quartz, 65% feldspar and 5% mica (Baldi et al., 1982, Jamiolkowki et al., 2003).

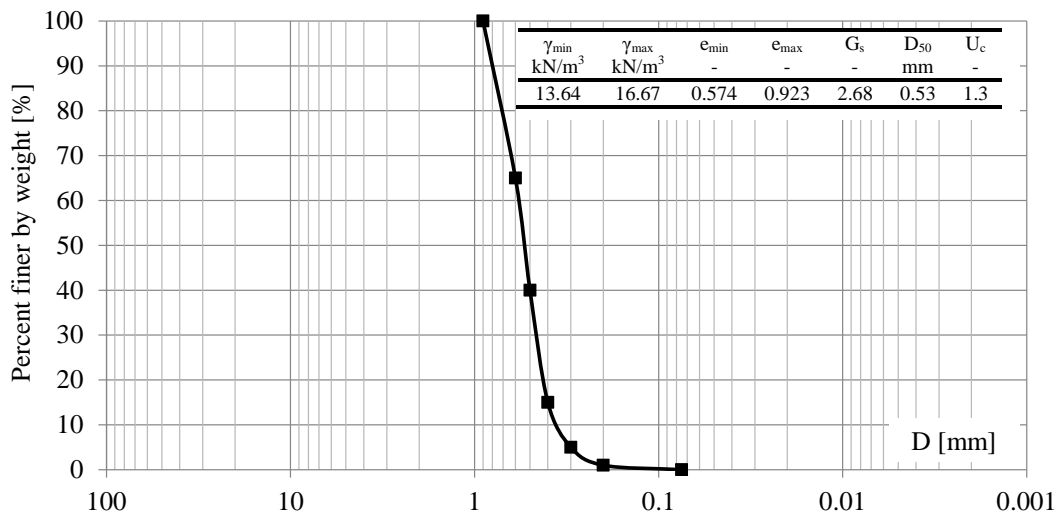


Figure 1. Grain size distribution and index properties of TS4

The model cone penetration tests were performed using the ISMGEO seismic geotechnical centrifuge (ISGC), which is a beam centrifuge made up of a symmetrical rotating arm with a diameter of 6 m, a height of 2 m and a width of 1 m, which gives it a nominal radius of 2 m. A 1-D shaking table is fixed at one end of the arm. The centrifuge has the potential of reaching an acceleration of 600g at a payload of 400 kg. The maximum dimensions of the model are: length = 1 m, height = 0.8 m, with = 0.5 m (Baldi et al., 1988).

The tests were carried out using a miniaturized electrical piezocone, which has a diameter $d_c = 11.3$ mm, an apex angle of 60° , a sleeve friction 11.3 mm in diameter and 37 mm long. The test program consisted of 27 centrifuge CPTs on dry TS4 models. Each soil model was reconstituted

at 1g to the target void ratio by pluviating in air the dry sand into a cylindrical container using a travelling sand spreader. The cylindrical container has an internal diameter of $D = 400$ mm, a height of 630 mm and rigid walls to avoid lateral displacements of the soil. The model container internal diameter was large enough to minimize rigid wall boundary effects, according to Bolton et al. (1999): container size effect, $D/d_c = 35.4 > 30$; side boundary effect, $s/d_c = 17.2 > 10$, where s is the distance of the cone shaft from the side wall. After the deposition, a very rigid frame, which held the piezocone, two linear displacement transducers (LDT) to monitor the cone displacement and the sand surface settlement, respectively, and a hydraulic actuator, was fixed to the container walls. Figure 2 shows a model scheme and a model picture.

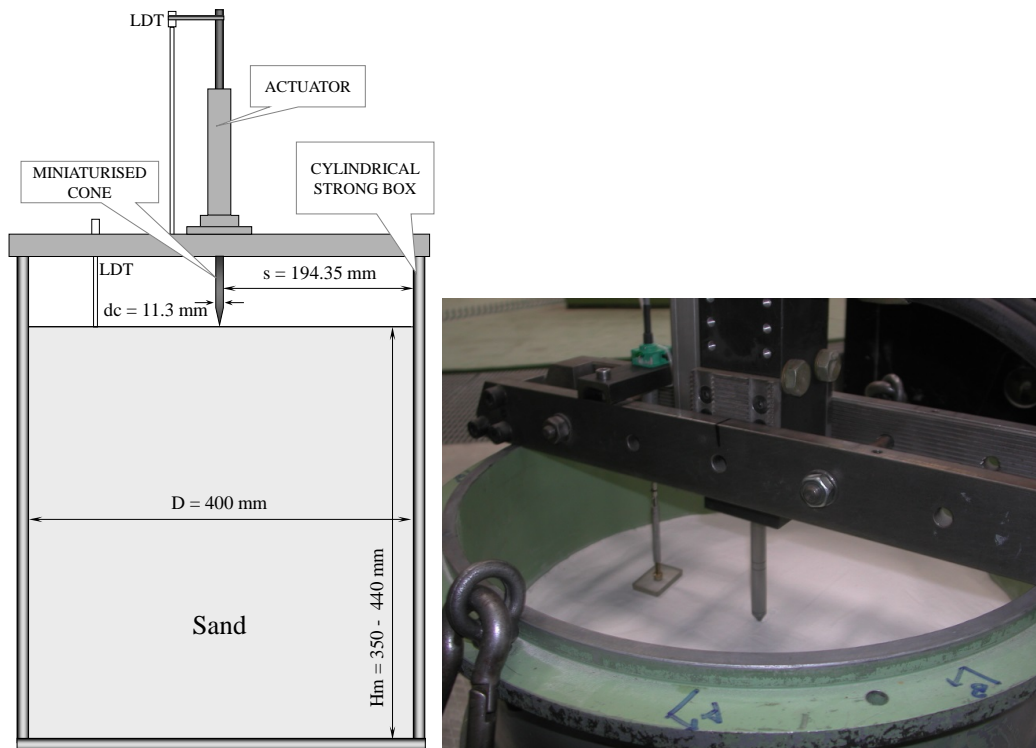


Figure 2. Model scheme and model picture

Each sand model was loaded in the centrifuge and accelerated to the target acceleration. As the model was subjected to the acceleration field in the centrifuge, the soil surface slightly settled due to the self-weight and the model compressed, as monitored by the LDT. When the surface settlements ended up, the cone penetration test was carried out applying a penetration rate of 2 mm/s. The test penetration was interrupted at $20d_c$ of distance from the container bottom to avoid rigid boundary effects (Bolton et al., 1999). Only one test per model was performed in the central axis of each sample accelerated at one target value. The model unit weight γ_{dry} , void ratio e and relative density D_R values refer to the end of in-flight compression and were assumed constant with depth in test interpretation.

To measure a q_c profile over a wide range of stresses, three acceleration levels were imposed by the centrifuge to soil models of the same dimensions: 30g, 50g and 80g, reproducing a stress range from about 30 to 300 kPa. In order to take into account the progressive mobilization of the

cone resistance from the model free surface (Schmertmann, 1978) the measures registered in the first $10d_c$ of penetration from the surface were removed. The results of centrifuge CPTs are shown in Figure 3, where the tip resistance q_c is plotted as a function of the mean effective stress $p' = (\sigma'_v + 2\sigma'_h)/3$ and the “operative” stress intervals reproduced by the acceleration levels are evidenced. The test results show that the soil models are rather homogeneous and the tests are repeatable so that the q_c values measured on models with similar void ratio subjected to different accelerations almost describe a unique cone resistance profile. The unavoidable scatter can be attributed to slight differences in void ratio among models.

For comparison and validation of the centrifuge tests, the results of CPTs on dry TS4 carried out in large calibration chamber (CC, soil specimen diameter = 1.2m, height = 1.5m) (Jamiolkowki et al., 2003) are also plotted in Figure 3; all the CC tests here reported were carried out on normally consolidated samples, subjected to a stress ratio equal to the value at rest and applying BC3 boundary conditions (constant vertical stress and prevented lateral displacement), which are the conditions most similar to the centrifuge tests. A good agreement between CC and centrifuge results was observed. Respect to CPTs in the large Calibration Chamber, those performed in centrifuge have the advantage of giving a whole q_c profile over a wide range of stresses, rather than a single q_c value associated to the specific values of the void ratio and the applied stress level of a single sample, but have the disadvantage of one fixed boundary condition.

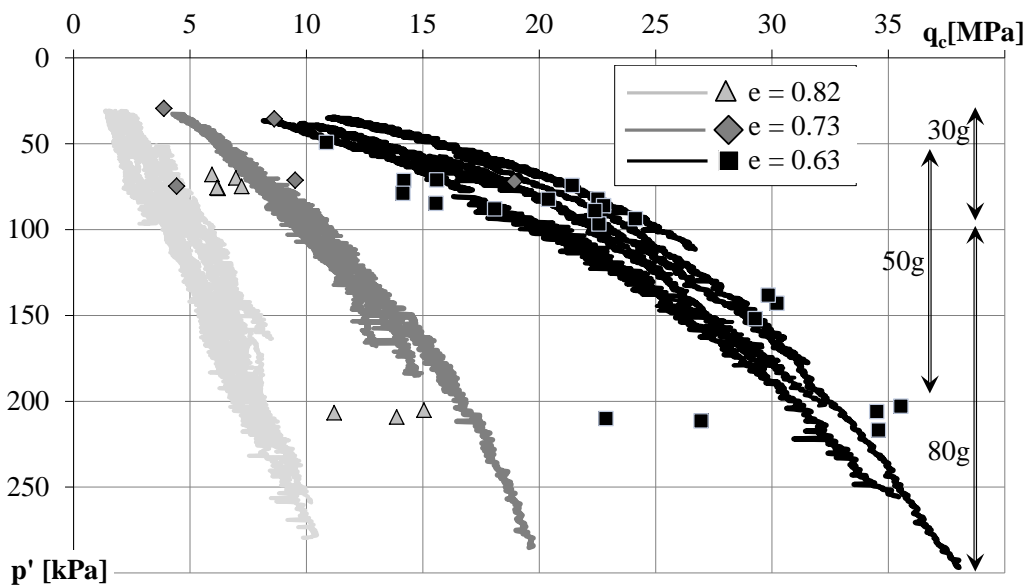


Figure 3. Tip resistance q_c as a function of mean effective stress p'

The centrifuge q_c curves in Figure 3 are re-plotted in Figure 4 after normalizing the tip resistance over p' : $Q_p = (q_c - p)/p'$. For each test, the values of the state parameter ψ at the starting point and at the end of the Q_p profiles are also indicated. The state parameter is defined, according to Been and Jefferies, 1986, as $\psi = e - e_{cs}$ where: e = current void ratio; e_{cs} = void ratio on the critical state line CSL (described below) at the same p' . It's worth noting that, assuming a constant void ratio with depth for the models, the state parameter increases as the penetration progresses (i.e. as the stress level increases). All the models were characterized by $\psi < 0$.

The normalized tip resistance Q_p from all the centrifuge CPTs is plotted as a function of the state parameter ψ in Figure 5. The $Q_p - \psi$ curves of TS4 can be interpolated with a unique trend-line which can be interpreted with the equation (Been et al., 1986):

$$Q_p = k e^{-m\psi} \quad (1)$$

where $m = 8.4$ and $k = 26.4$ are dimensionless fitting parameters.

It is very similar to the trend indicated by Jefferies and Been, 2006 for Ticino Sand on the base of calibration chamber tests.

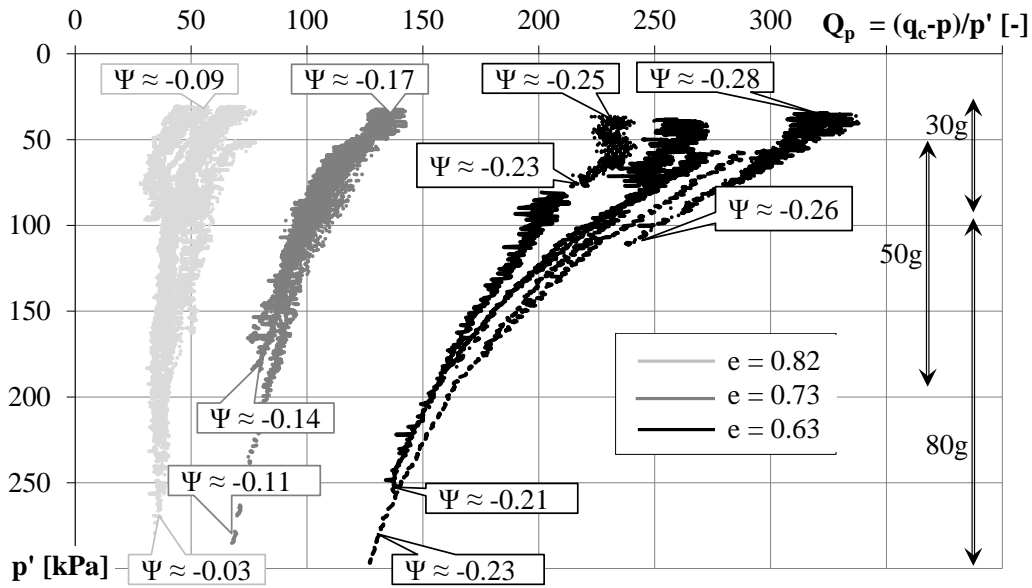


Figure 4. Normalized tip resistance Q_p as a function of mean effective stress p'

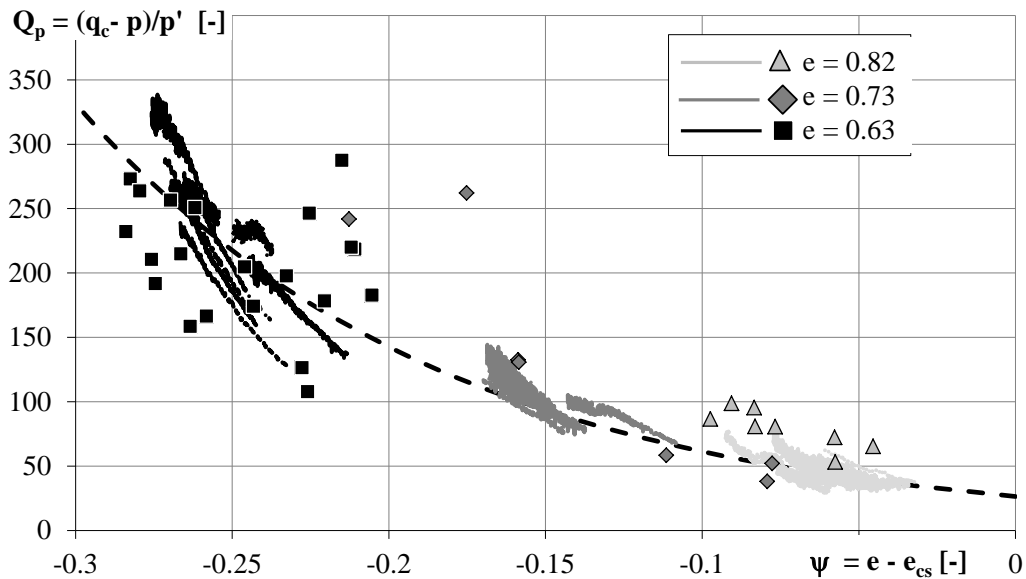


Figure 5. Normalized tip resistance Q_p as a function of the state parameter ψ

Monotonic and Cyclic Behavior of TS4

The mechanical behavior of TS4 was investigated through a series of monotonic and cyclic Tx tests selected from a large database of tests performed at the ISMGEO laboratory. All the tests were carried out on samples reconstituted by pluvial deposition in air of the dry sand, subsequently saturated.

The monotonic tests consisted in Tx compression on both isotropic and anisotropic consolidated samples. The applied consolidation mean effective stress p'_c ranged from 50 to 870 kPa. The samples were both normally consolidated and over consolidated. The failure was reached applying standard drained and undrained compression stress paths ($\Delta\sigma_a > 0$ and $\Delta\sigma_r = 0$). The states of the samples at critical states were fitted with a power law (according to Li & Wang, 1998) as follows: $e_{cs} = \Gamma - \lambda(p'/p_{ref})^\alpha$, where: $p' = (\sigma'_a + 2\sigma'_r)/3$ = mean effective stress; $p'_{ref} = 101$ kPa = atmospheric pressure; Γ , λ , α = material constants determining the critical state line position and shape, whose values were obtained from data best fitting: $\Gamma = 0.923$; $\lambda = 0.046$, $\alpha = 0.5$. The stress ratio at critical state M_c resulted equal to 1.36, which corresponds to a critical state angle $\varphi'_{cv} = 34^\circ$.

The undrained cyclic Tx tests on TS4 were performed on reconstituted samples, isotropically normally consolidated at a mean effective stress $p'_c = 100$ kPa. Only to one samples was applied an isotropic pressure of 200 kPa. A direct consequence of testing at same p'_c is that making reference to the density of the specimens is equivalent to making reference to the average state parameter, ψ_{avg} . The tested specimens were reconstituted at three values of void ratio: medium void ratio ($e_{avg} = 0.742$, which corresponds to $\psi_{avg} = -0.132$), low void ratio ($e_{avg} = 0.676$, $\psi_{avg} = -0.201$) and very low void ratio ($e_{avg} = 0.582$, $\psi_{avg} = -0.295$). The states of all the samples laid below the CSL, i.e. at the end of the consolidation all the specimens had $\psi < 0$.

Figures 6a – 6d show the results of the test TS4_13_8 in terms of: axial deformation ε_a vs. the number of cycles N (Figure 6a); deviatoric stress q vs. ε_a (Figure 6b); excess pore pressure Δu vs. N (Figure 6c); q vs. mean effective stress p' (Figure 6d). The sample was subjected to a stress deviator $\Delta q = \Delta\sigma_a = \pm 62$ kPa ($CSR^{TX} = \Delta q/2p'_c = 0.31$). During the test, the specimen undergoes a typical response known as “cyclic mobility”. Axial strains and pore pressure build up gradually during each cycle, as the effective stress p' reduces. Failure or liquefaction condition, assumed as the condition at which $\varepsilon_a^{DA} = 5\%$, was reached between the 14th and 15th cycles and it is evidenced with an empty circle in the Figures. At this point $\Delta u \approx 90$ kPa and the pore pressure ratio is $R_u = \Delta u/p'_c \approx 0.9$.

All the failure conditions of the tested samples are represented in Figure 7; in this Figure the applied cyclic stress ratio CSR^{TX} is corrected for simple shear conditions: $CSR^{SS} = CSR^{TX}(1+2K_0)/3$, where $K_0 = \sigma'_h/\sigma'_v$ is the stress ratio at rest, computed as a function of φ'_{cv} . The cyclic resistance of medium void ratio samples ($\psi_{avg} = -0.132$) is represented by empty circles, that of dense sample ($\psi_{avg} = -0.201$) by full squares, that of very dense samples ($\psi_{avg} = -0.295$) by grey triangles. The three groups of samples have a similar behavioral trend, which can be interpreted with a power functions, as shown in Figure 7.

Liquefaction Assessment

At the reference number of cycles $N = 15$, the cyclic resistance ratio of the three groups of samples of Figure 7 is: $CRR_{15}^{SS} = 0.12, 0.16$ and 0.41 , respectively. These values are plotted in Figure 8 as a function of Q_p , computed using Eq. 1 from the three values of ψ . A preliminary fitting line has been drawn, which defines two areas, the one below the curve where liquefaction is not expected, the other above where liquefaction is possible.

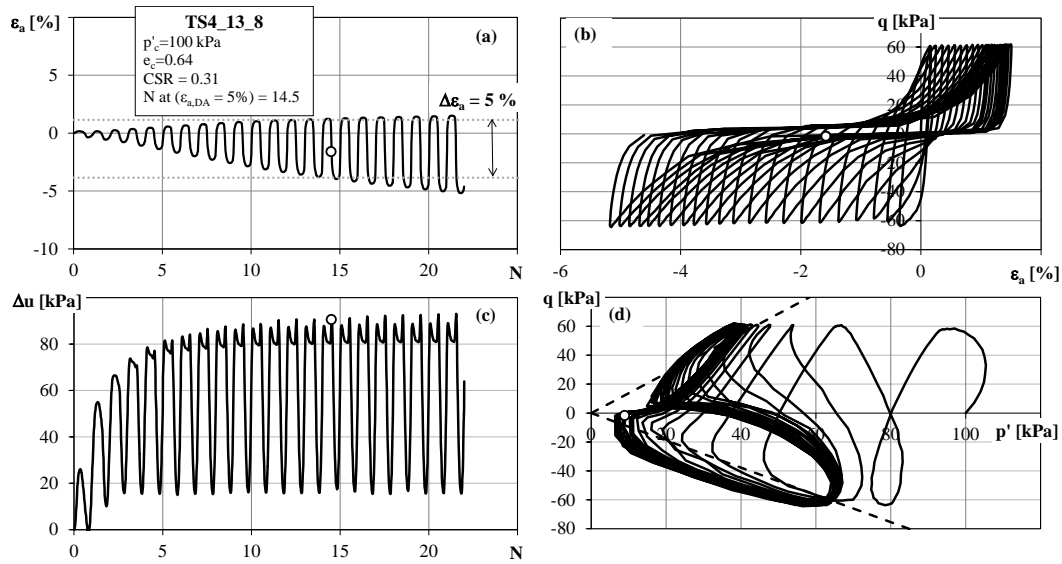


Figure 6. Cyclic triaxial test TS4_13_8: (a) axial strain ϵ_a vs. number of cycles N ; (b) stress deviator q vs. ϵ_a ; (c) excess pore pressure Δu vs. N ; (d) q vs. mean effective stress.

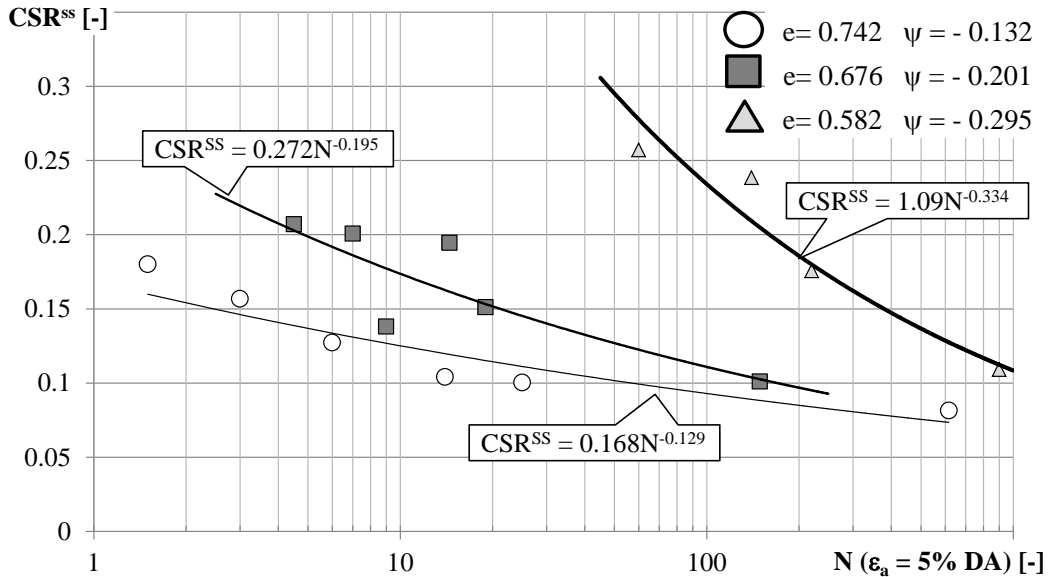


Figure 7. Cyclic strength of TS4 in simple shear conditions

Conclusions

The aim of the paper is to introduce an alternative method for evaluating the cyclic resistance of an un-aged, un-cemented sand, from the results of cone penetration tests, based on the state parameter. The normalised tip resistance Q_p was deduced from CPTs performed in centrifuge with a miniaturised piezocone on homogeneous reconstituted models, while the undrained cyclic resistance was achieved through undrained cyclic tests on reconstituted specimens of Ticino sand. Relationships between Q_p and ψ , CRR and ψ , have been defined, to allow the direct estimation of CRR_{15} from Q_p . A correlation usable in the engineering practice will require a calibration on a wider number of sands and a validation on sites where liquefaction occurred.

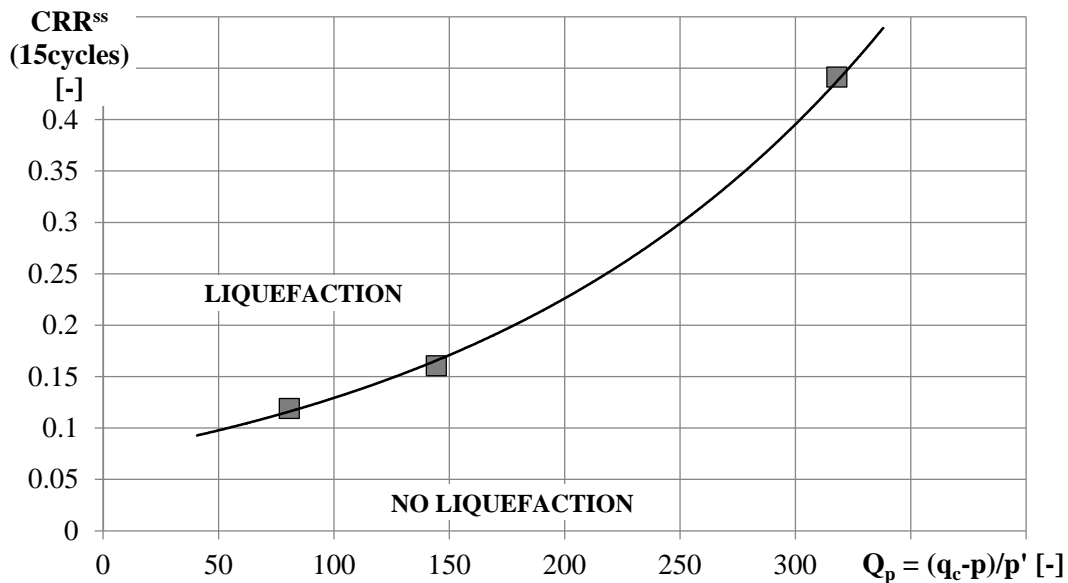


Figure 8. Cyclic resistance ratio at 15 cycles for simple shear conditions CRR_{15}^{SS} vs normalized cone resistance Q_p

References

- Andrus R. D. and Stokoe II K. H., (1997). Liquefaction resistance based on shear wave velocity. Evaluation of liquefaction resistance of soils. *National Center for Earthquake Engineering Research (NCEER) Workshop*. Proceedings. January 5-6, 1996, Salt Lake, UT, Youd, T.L. Idriss I.M. Editors pp. 89-128.
- Baldi, G., Bellotti, R., Ghionna, V., Jamiolkowski, M. and Pasqualini, E. (1982); Design parameters for sand from CPT. *Proc. ESOPT 2*, Amsterdam.
- Baldi, G., Belloni, G., Maggioni, W. (1988). The ISMES Geotechnical Centrifuge. In *Centrifuge 88*, Paris, Corté J. F. Ed., Balkema, Rotterdam, pp. 45-48.
- Been, K. and Jefferies, M.G. (1985). A state parameter for sands. *Géotechnique*, **35**, 2, 99–112.
- Been, K., Crooks, J.H.A., Becker, D.E. and Jefferies, M.G. (1986). The cone penetration test in sands: Part I, state parameter interpretation. *Géotechnique*, **36**, 2, 239–249.
- Bolton, M.D., Gui, M. W., Garnier, J., Corte, J. F., Bagge, G., Laue, J. & Renzi, R. (1999). Centrifuge Cone Penetration Tests in Sand. *Geotechnique*, Vol. **49**, No. 4, pp. 543-552.
- Jamiolkowski, M.B., Lo Presti, D.C.F., Manassero, M. (2003). Evaluation of Relative Density and Shear Strength

from CPT and DMT. *Soil Behavior and Soft Ground Construction*, Ladd Symposium, MIT, Cambridge Mass. Geotechnical Special Publication No. 119, Germaine J.T., Sheahan, T.C., Whitman, R.V. Eds., pp. 201-238.

Jefferies, M and Been, K. (2006). *Soil liquefaction. A critical state approach*. Taylor and Francis, London.

Li, X.-S., and Wang, Z.-L. (1998); Linear representation of steady state line for sand. *Journal of Geotechnical and Geoenvironmental Engineering*, ASCE, **124**, 12, 1215–1217.

Robertson, P.K., and Campanella, R.G. (1985); Liquefaction potential of sands using the cone penetration test. *Journal of Geotechnical Engineering Division*, ASCE, **22**, GT3, 298–307.

Schmertmann, J.H. 1978. *Guidelines for Cone Penetration Test, Performance and Design*, Report FHWA-TS-787-209, Federal Highway Administration, Washington, July 1978, 145 pgs.

Seed, H. B., and Idriss, I. M. (1982). “*Ground motions and soil liquefaction during earthquakes.*” Earthquake Engineering Research Institute Monograph, Oakland, Calif.